Silicon Torsional Scanning Mirror

Conventional batch photolithography and thin film techniques are employed to fabricate an electrostatically driven torsional scanning mirror from single-crystal silicon. This device is extremely simple to make and operate, has operational characteristics comparable to commercial magnetically driven high-frequency scanners, and has exhibited a promising reliability.

Introduction

Never have the severe demands of high technology been felt more keenly than in the area of today's small, highprecision mechanical devices. Solid state laser and fiber optic mounts and couplings [1], ink jet nozzles [2] and charge plates [3], magnetic disk read/write heads, and optical recording heads are all examples of mechanical components requiring submicron dimensional control and/or submicron system positioning accuracy. Since modern thin film techniques are inherently accurate to such dimensions, it is not surprising that these and other miniature mechanical design questions have been turning more and more to thin film materials and thin film processing methods including photolithography, sputter deposition and etching, plasma processing, and single-crystal silicon anisotropic etching for high-precision, low-cost answers.

Many applications of high-precision mechanical devices fall into the category of movable head structures such as print heads, magnetic heads, and optical recording heads. Because they are movable, these components are subject to the additional restrictions of compactness and light weight since the heads must be accelerated and moved rapidly across a surface. Again, thin film and silicon processing technology seems ideally suited to these applications since the structures fabricated with these techniques are inherently small, lightweight, rugged, and reliable. A further important advantage is that the design of the mechanical/electronic interface can be significantly facilitated by utilizing thin film procedures since they are fundamentally compatible with silicon integrated circuit fabrication procedures.

The device described here is a new micromechanical structure which demonstrates many of the advantages of using thin film and silicon processing materials and techniques in mechanical applications. Not only is the design and fabrication of the silicon torsional scanning mirror much simplified and less expensive compared to conventional mechanical scanners, but the operation of this device is found to be comparable to that of those conventional scanners, and even more importantly, initial results suggest that this device should be just as reliable. In addition, the versatility in design and the future extendibility of these fabrication techniques make the technology very attractive.

Basically, the structure consists of two pieces. The single-crystal silicon chip contains a mirror element attached to two single-crystal silicon torsion bars, as shown in Fig. 1. This silicon chip is bonded to another substrate (glass or silicon) into which a shallow rectangular well has been etched. At the bottom of the well are two electrodes which are alternately energized to deflect the mirror element in a torsional movement about the silicon torsion bars. A ridge in the middle of the well was found to be necessary to prohibit transverse oscillations of the mirror.

The following sections of this paper will describe fabrication procedures, calculated and observed operational characteristics, and reliability behavior. In addition, the electrostatic silicon torsion mirror will be compared to conventional commercial devices performing the same function.

Copyright 1980 by International Business Machines Corporation. Copying is permitted without payment of royalty provided that (1) each reproduction is done without alteration and (2) the *Journal* reference and IBM copyright notice are included on the first page. The title and abstract may be used without further permission in computer-based and other information-service systems. Permission to *republish* other excerpts should be obtained from the Editor.

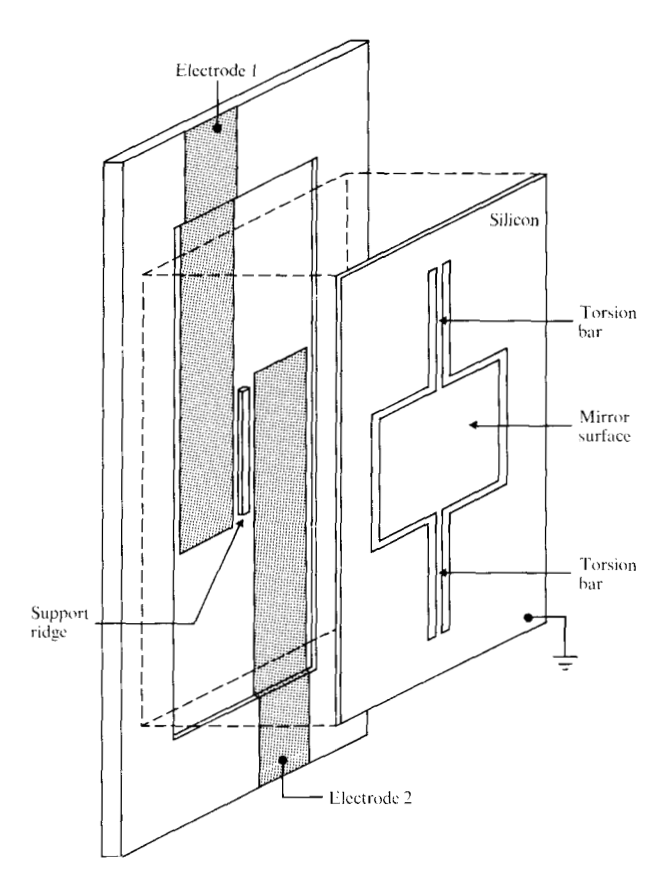


Figure 1 Exploded view of silicon torsion mirror structure showing the etched well, support ridge, and evaporated electrodes on the glass substrate.

Fabrication

The present design of the silicon torsional scanning mirror consists of only two pieces, the silicon chip processed with a single mask level and the glass substrate processed with two mask levels. Fabrication proceeds as follows:

- 1. Oxidize the 134- μ m-thick silicon wafer ($\approx 0.5 \ \mu$ m SiO₉).
- 2. Using Mask 1, etch away the SiO₂ in the regions shown in Fig. 2(a).
- 3. Etch the exposed silicon in the anisotropic etchant ethylene diamine, pyrocatechol, and water (EDP) clear through the wafer.
- 4. Strip the first oxide layer and reoxidize ($\approx 1 \mu m$). The silicon now appears as shown in Fig. 3.
- 5. Evaporate an aluminum reflecting layer on the surface of the central mirror element.
- 6. Sputter a Cr-Au masking layer on the surface of a glass slide (≈2.5 × 1.5 cm).
- 7. Etch the Cr-Au layer with the pattern shown in Fig. 2(b).

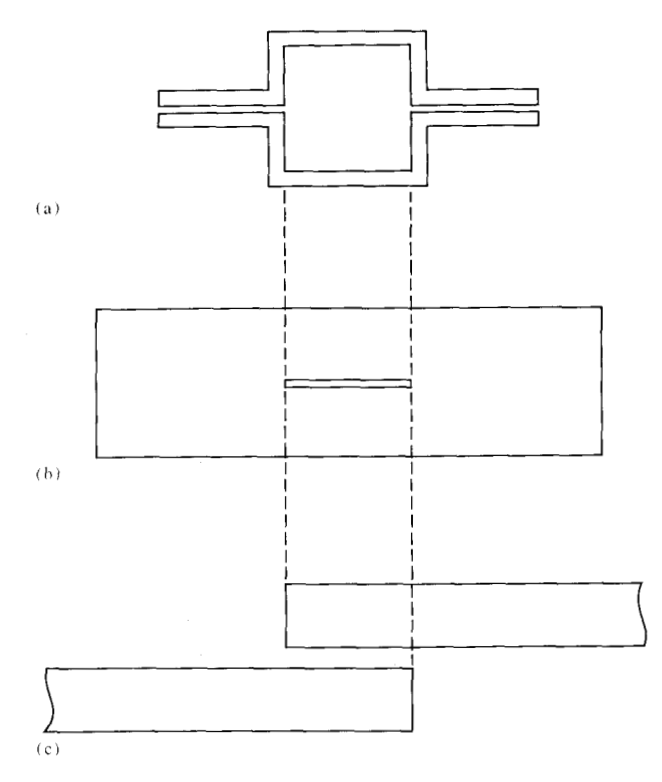


Figure 2 The three masks used to fabricate the mirror structure. (a) Mask 1 (silicon) is used on the silicon, (b) Mask 2 (well) and (c) Mask 3 (electrodes) are used on the glass substrate.

- 8. Etch the glass in buffered HF (6:1) to a depth of 7-10 μ m (etch rate $\approx 1 \mu$ m/min).
- 9. Strip off first Cr-Au layer and deposit another ($\approx 0.02 \, \mu \text{m}$ Cr, 0.1 μm Au).
- 10. Etch the second Cr-Au layer into two electrodes as shown in Fig. 2(c).
- 11. Align the two pieces and bond, as shown in Fig. 1.
- 12. Attach wires to the two electrodes and to a region of the silicon from which the SiO₂ has been removed.

The primary advantage of this fabrication procedure is batch processing of a simple two-component assembly. In particular, over fifty pieces of the 15-kHz device described here could easily be etched from a single 57.2-mm (2 1/4-inch) silicon wafer, while thirty etch glass substrates could be cut from a single 51 \times 51-mm (2 \times 2-inch) processed glass plate.

Several long-term advantages of the use of silicon in this application are also anticipated. In particular, portions of the driving or position-sensing circuitry might be fabricated on the same piece of silicon; or field-assisted bonding [4] might be employed to bond an entire processed wafer to a processed glass plate, cutting up the

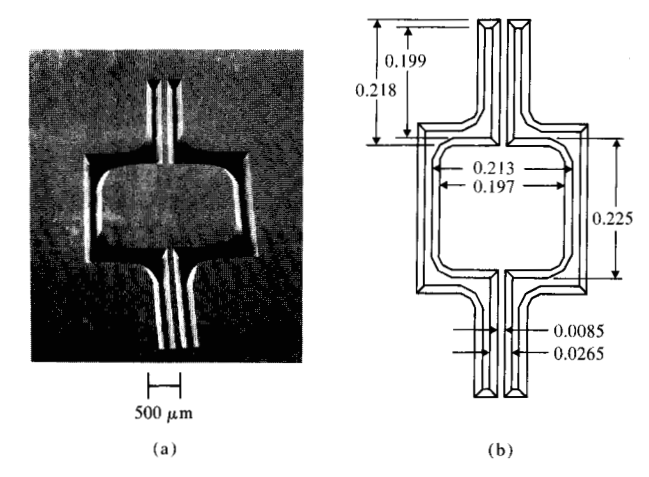


Figure 3 (a) SEM of typical torsion mirror (tilted 60°) and (b) measured dimensions of 15-kHz mirror (in cm) of typical mirror element. The SEM photo is a view of the mirror from the back surface where the electrostatic fields are applied.

assembly into individual devices afterwards. Finally, novel geometrical extensions can be expected such as multiple mirrors on a single substrate for both x and y deflection.

Calculations

Determination of the operational parameters of the electrostatically deflected silicon torsional mirror is relatively straightforward. The torsional resonant frequency of the vibrating structure is given by [5]

$$f_{\rm R} = \frac{1}{2\pi} \sqrt{\frac{JG}{I(l/2)}} ,$$
 (1)

where J is the polar moment of inertia of the silicon shaft, G is the shearing modulus of elasticity of the silicon, I is the moment of inertia of the mirror itself, and I is the length of the silicon torsion shaft. The polar moment of the inertia of the shaft is represented by $J = Kt^4$, where K is a constant depending on the cross-sectional shape of the shaft [6], and t is the thickness of the wafer as shown in Fig. 4. For simple cross sections, the ratio J/A^2 (where A is the cross-sectional area of the shaft) lies between 0.11 and 0.16 and is estimated to be about 0.13 for the complex shape here, which corresponds to K = 0.24. Equation (1) can now be expressed as

$$f_{\rm R} = \frac{1}{2\pi} \sqrt{\frac{12KEt^3}{\rho lb^4(1+\nu)}} \,, \tag{2}$$

since $I = \rho b^4 t/12$, where ρ is the density of silicon (2.32 gr/cm³), b is the width (and length) of the square mirror, and $G = E/2(1 + \nu)$, where E is Young's modulus

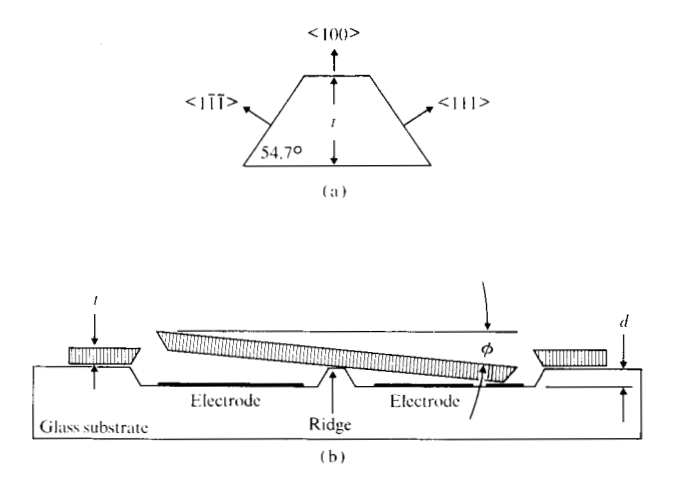


Figure 4 (a) Cross section of anisotropically etched torsion bar where $t = 134 \, \mu \text{m}$. (b) Cross section of mirror element defining the deflection angle $\phi(d = 12.5 \, \mu \text{m})$.

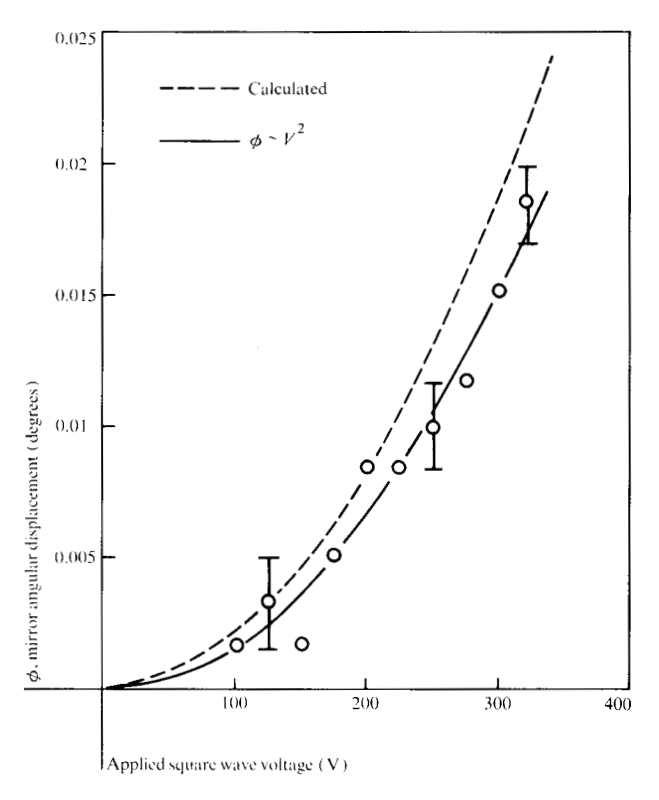


Figure 5 Calculated and experimental off-resonance deflection of torsion mirror as a function of square wave voltage.

 $(1.9 \times 10^{11} \text{ Pa})$ and v is Poisson's ratio (0.09). For the parameters given in Fig. 3, we calculate $f_{\rm R}=16.3$ kHz, compared to the experimental value of 15 kHz.

Deflection amplitudes of the torsion mirror as a function of voltage can be readily determined well below reso-

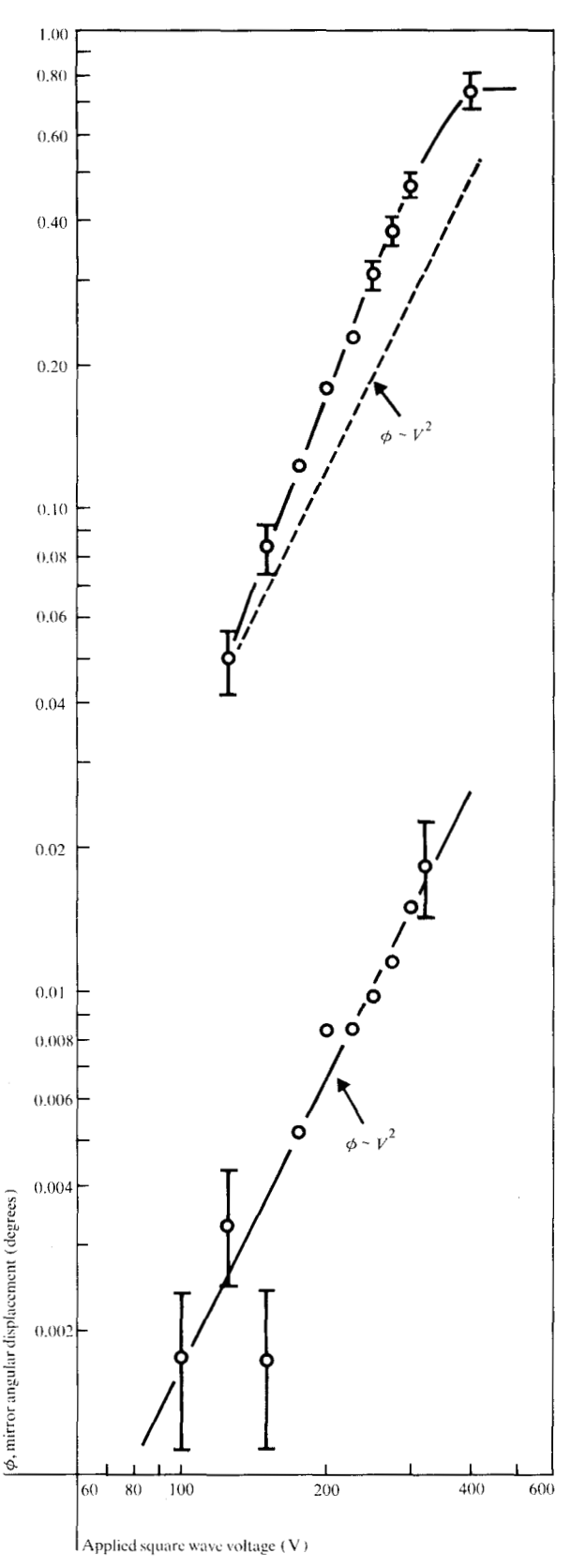


Figure 6 Experimental deflections of torsion mirror. Resonant displacements are shown at the top, off-resonance at the bottom. Note departure from square law dependence at the top.

nance. Total torque on the mirror element is calculated by integrating the incremental torque over the half segment of the mirror which is being electrostatically attracted by a single bottom electrode:

$$T = \int_0^{b/2} F(x)x dx,\tag{3}$$

where the electrostatic force is determined by the distance between the bottom of the mirror segment and the electrode, $d(x) = d - \phi x$. Here, ϕ is the angle of rotation of the mirror as indicated in Fig. 4:

$$T = \frac{1}{2} \varepsilon_0 V^2 b \int_0^{b/2} \frac{x dx}{(d - \phi x)^2}$$
$$= \frac{\varepsilon_0 V^2 b}{2\phi^2} \left[\ln \left(1 - \frac{\phi b}{2d} \right) + \frac{\phi b/2d}{1 - \phi b/2d} \right]. \tag{4}$$

For high-resonant-frequency mirrors ($\gtrsim 10 \text{ kHz}$), Q factors are relatively high (>10), so that the off-resonance angular displacement is small compared to $\phi_{\text{max}} = 2d/b$ (the maximum possible deflection angle of the mirror). Under these conditions Eq. (4) can be approximated

$$T = \frac{\varepsilon_0 V^2 b^3}{16d^2} \ . \tag{5}$$

Now a torque T on a shaft causes an angular twist in the shaft $\lceil 5 \rceil$

$$\phi = \frac{T(l/2)}{G(Kt^4)} \ . \tag{6}$$

Combining Eqs. (5) and (6), we find

$$\phi = \frac{\varepsilon_0 V^2 l b^3 (1 + \nu)}{16 \ K E d^2 t^4} A,\tag{7}$$

for $\phi << \phi_{\rm max}$ at frequencies far below resonance, where A is an areal correction factor $(A\approx 0.8)$, since the active bottom electrode area does not completely correlate with exactly one-half the torsion mirror area (due to rounded mirror corners and the absence of electrode metallization near the central ridge). Again, for the parameters given in Fig. 5 we calculate the dashed line of Fig. 6, in good agreement with experiment.

Complex damping mechanisms, including viscous airdamping, proximity effects due to the closely spaced electrode, and mechanical damping of the material itself, are all active at the resonant frequency [7] and complicate calculations at this point. In addition, at large deflection angles, nonlinear forces become important, as seen in Eq. (4), and the deflection amplitude is no longer quadratic with the voltage (see Fig. 6). For these reasons, no calculations will be attempted in this regime. In a qualitative fashion, however, while the *intrinsic* mechanical Q of such a structure would be expected to be high, both vis-

cous air-damping and the proximity of the substrate tend to lower this intrinsic value by about an order of magnitude [7]. The relatively low Q values of about 20 which have been observed, then, are not surprising. Future structures, however, can be designed to minimize air damping losses, for example, by etching deeper wells and by using support posts instead of ridges to permit freer flow of air.

Reliability of such a vibrating structure depends on the total maximum stress encountered at the point of maximum torque. The maximum stress of a shaft with an equilateral triangular cross section occurs at the midpoint of each side and is given by [6]

$$\tau_{\text{max}} = \frac{30.8 \ T_{\text{max}}}{(t')^3} \approx \frac{9.5 \ T_{\text{max}}}{t^3},$$
(8)

where t' is the height of the triangle and t is the actual thickness of the silicon $(t \approx 2t'/3)$ for the cross section in Fig. 4. Maximum torque is found from Eq. (6), substituting $\phi = \phi_{\text{max}} = 2d/b$:

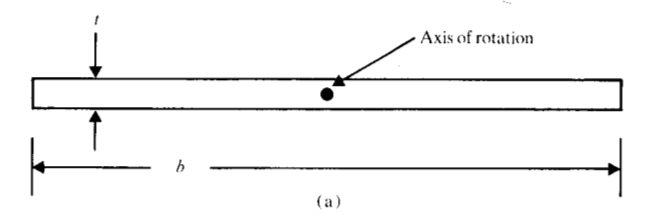
$$\tau_{\text{max}} = \frac{38KE}{2(1+\nu)} \left(\frac{dt}{bl}\right). \tag{9}$$

For the dimensions described here, this corresponds to about 3.0×10^8 Pa, or nearly ten times smaller than the fracture stresses found by Pearson *et al.* [8] for bending movements in thin silicon rods and whiskers at room temperature. Reliability, then, is expected to be high, as will be discussed later.

Finally, high-precision optical scanning systems require elements with very low distortion. This can be a severe problem in high-speed vibrating mirrors since the dynamic torque produces a surface distortion at the flyback position where the angular acceleration is greatest. The distortion δ is illustrated in Fig. 7 and is given by [9]

$$\delta = (0.226) \left(\frac{\rho}{E} \right) \frac{b^5}{t^2} 2\phi_{\text{max}} f^2 (1 - \nu^2). \tag{10}$$

For the structure described here with f=15 kHz, we find $\delta=30$ nm, or about $\lambda/20$, at 632.8 nm. More generally, however, silicon has an intrinsic advantage (in terms of distortion) over conventional materials used as torsional mirrors (quartz or glass) since the ratio (ρ/E) is almost three times smaller in silicon than in quartz [10, 11]. For the same mirror dimensions and operating parameters, then, silicon will typically exhibit about one-third the distortion of quartz. Indeed, some special-purpose scanners can now be purchased which are fitted with passive mirror elements cut from single-crystal silicon.



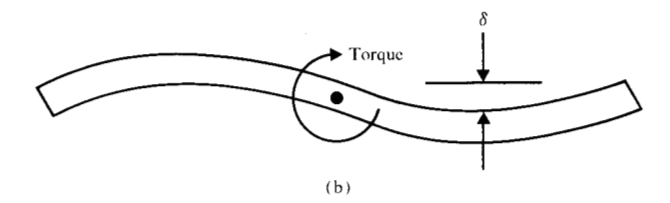


Figure 7 Distortions of a mirror substrate due to high dynamic torque. Mirror cross section (a) in equilibrium and (b) under torque.

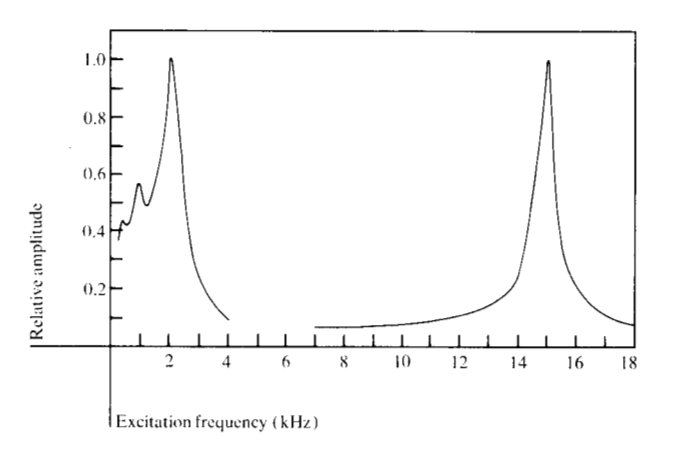


Figure 8 Deflection amplitude vs. drive frequency for two mirrors with differing resonant frequencies.

Operation

Implementation of the electrostatically driven torsion mirror is extremely simple, partially because the power consumed is so small. In the experiments here, low-voltage square wave oscillators coupled into a small audio step-up transformer were used to drive the mirrors. Since the deflection mechanism is purely electrostatic and involves primarily the charging and discharging of small capacitors, power dissipation is minimal and occurs mainly in the driving circuitry (typically ≈100 mW) even though the deflection voltages are large, 300-400 V. Off-resonance scanning does not seem to be practical because of the extremely high voltages which would be required as seen by extrapolating the lower, off-resonance deflection

Table 1 Comparison of resonant scanning mirrors.

	Silicon mirror Batch fabrication of two photolithographically processed plates		Complex mechanical assembly of many parts		Piezoelectric Two bonded ceramic plates with separate mirror attached	
Fabrication procedure Frequency scan angle						
	15 kHz ±1°	$\begin{bmatrix} 50 \text{ kHz} \\ \pm 2^{\circ} \end{bmatrix}^*$	1 kHz ±30°	15 kHz ±2°	1 kHz ±5°	40 kHz ±0.1°
Power	<0.1 W dissipated in drive circuitry		≈0.5 W dissipated in assembly		<0.1 W dissipated in drive circuitry	
Relative distortion	1/3 (silicon mirror)		1 (quartz mirror)		1 (quartz mirror)	
Reliability	≈10 ¹² cycles demonstrated		Very high		Very high	
Other	High voltage		High power Heavy assembly		High voltage Off-axis mirror Creep and hysteresis	

^{*}Projected performance.

curve in Fig. 6. Typical deflection amplitude vs. frequency is illustrated in Fig. 8 for two mirrors resonant at 2 kHz and 15 kHz, exhibiting Q's of about 3 and 25, respectively.

Perhaps the most serious question which should be raised concerning the operation of the device described here is that of reliability. That is, can a single-crystal silicon structure, which has been anisotropically etched to reveal highly angular, stress-concentrating facets, be subjected to large dynamic stresses continuously over long periods of time without fatigue and/or failure? Although previous static stress studies [8] suggested that singlecrystal silicon can exhibit yielding strengths comparable to those of high-strength nickel-alloy steel, this material has never before been asked to withstand the extreme conditions encountered in a high-speed torsional mirror, including peak accelerations of over $3.4 \times 10^4 \text{ m/s}^2$ (3500 G's) and dynamic stresses in the shaft of over 3.0×10^8 Pa (42 000 psi) 30 000 times a second! For these reasons, much of this study concentrated on preliminary life-tests of these devices.

Several samples have been tested. Although the highly angular facets which result from anisotropic etching can be smoothed by several methods [12], it was decided not to smooth initially, as a worst-case test. None of the four devices tested showed any observable changes in operating characteristics, including the most recent design, a 2-mm-square mirror resonating at 35 kHz, scanning ± 0.28 degrees nearly 10^{12} cycles (250 days). An enhanced dislocation density and some stress-cracking found in

early devices were attributed to errors in fabrication such as 1) improper over-etching which left additional stress concentration regions due to drastic undercutting and 2) improper glass/silicon bonding which allowed unwanted transverse oscillations of the assembly. An additional early problem, arcing between the silicon and the Cr electrodes, was solved by oxidizing the silicon after the EDP etch and sputter-depositing SiO_2 over the patterned Cr electrodes.

There are additional, fundamental reasons why singlecrystal silicon should exhibit a high fatigue strength. It is well known that the initiation of fatigue cracks occurs primarily at free surfaces where stresses are highest and surface imperfections can cause additional stress concentration regions and the growth of microcracks [13]. Since etched silicon surfaces can be extremely flat with low defect and dislocation damage to begin with, single-crystal structures with etched surfaces would be expected to possess increased fatigue strength. In particular, Pearson et al. measured yield strengths on small etched single crystals greater than 2.0×10^9 Pa. At the same time, the microcracks which do develop at surface dislocations and defects typically grow during the portions of the stress cycle which produce tension at the surface of the material. By placing the immediate surface of a mechanical component under constant, uniform compression, then, enhanced fatigue strengths of metals have been observed. In the case of silicon, thin films of CVD Si₂N₄ are known to be in tension as deposited, putting the immediate silicon surface in compression. Such films may enhance the overall strength of a single-crystal silicon structure since the outer layer of silicon will remain in compression even if small flaws develop in this thin film coating.

Discussion

This paper describes the fabrication and successful operation of a new concept in torsional scanning mirrors. Nevertheless, the practicality and commercial viability of this device must be judged by comparing its characteristics with those of conventional magnetically and piezoelectrically driven torsional scanners. Table 1 compares the three devices in several important areas and shows some extrapolated projections of silicon mirror operational parameters. It is clear that silicon torsion mirrors offer substantial advantages in cost, ease of fabrication, weight, power dissipation, and distortion over electromagnetic assemblies at high scanning frequencies (≥15 kHz). These advantages are not maintained, of course, at low scanning frequencies. The silicon devices seem particularly applicable in functions which require compactness, light weight, and/or portability.

Several advantageous features of a silicon torsional scanning mirror are somewhat less obvious but important nonetheless. It should be noted, in particular, that highoptical-quality polished silicon wafers are standard in the semiconductor industry, are very readily available, and, in fact, can even be less expensive than quartz of similar optical quality. In addition, the fabrication concept described here is incredibly versatile. By a simple mask change, complex "ganged" scanning structures can be built, including an integral dual-mirror x-y scanner and multiple mirrors driven together for increasing total scan angle: increased versatility, designability, and complexity for no extra cost. Finally, the use of silicon, not only as the mirror element but also potentially as the substrate, makes it possible, at some future date, to include some of the driving as well as position-sensing circuitry integrated with the mirror structure.

The applications of such a torsional scanning mirror range anywhere from a dither function in optical recording head assemblies, in which light weight and low power are important, to laboratory fast-scanning instruments. The successful implementation and preliminary encour-

aging reliability behavior of this device may stimulate further uses of silicon not only as an electronic but also as a mechanical engineering material.

Acknowledgments

The author would like to thank A. Shartel, L. Holland, F. Anger, and J. Delaney for technical assistance and V. Hanchett for the SEM photograph.

References

- J. D. Crow, L. D. Comerford, R. A. Laff, M. J. Brady, and J. S. Harper, "GaAs Laser Array Package," Opt. Lett. 1, 40 (1977).
- E. Bassous, H. H. Taub, and L. Kuhn, "Ink Jet Printing Nozzle Arrays Etched in Silicon," Appl. Phys. Lett. 31, 135 (1977).
- L. Kuhn, E. Bassous, and R. Lane, "Silicon Charge Electrode Array for Ink Jet Printing," *IEEE Trans. Electron Devices* ED-25, 1257 (1978).
- G. Wallis and D. I. Pomerantz, "Field Assisted Glass-Metal Sealing," J. Appl. Phys. 40, 3946 (1969).
- A. Higdon and W. D. Stiles, Engineering Mechanics, Volume II: Dynamics, Prentice-Hall Inc., Englewood Cliffs, NJ, 1961, pp. 555-556.
- R. J. Roark and W. C. Young, Formulas for Stress and Strain, McGraw-Hill Book Co., Inc., New York, 1975, pp. 290-291.
- 7. W. E. Newell, "Miniaturization of Tuning Forks," Science 161, 1320 (1968).
- G. L. Pearson, W. T. Read, Jr., and W. L. Feldmann, "Deformation and Fracture of Small Silicon Crystals," Acta Met. 5, 181 (1957).
- 9. P. J. Brosens, "Dynamic Mirror Distortions in Optical Scanning," Appl. Opt. 11, 2987 (1972).
- H. F. Wolf, Silicon Semiconductor Data, Pergamon Press, Inc., Elmsford, NY, 1969.
- W. B. Hillig, "Strength of Bulk Fused Quartz," J. Appl. Phys. 32, 741 (1960).
- E. Bassous and E. F. Baran, "The Fabrication of High Precision Nozzles by the Anisotropic Etching of (100) Silicon,"
 J. Electrochem. Soc. 125, 1321 (1978).
- G. M. Sinclair and C. E. Feltner, "Fatigue Strength of Crystalline Solids," *Properties of Crystalline Solids*, 63rd Meeting of ASTM, American Society for Testing and Materials, Philadelphia, PA, 1960.

Received March 17, 1980; revised April 30, 1980

The author is located at the IBM Research Division laboratory, 5600 Cottle Road, San Jose, California 95193.